Advances in Automotive Engineering, *Vol. 1, No. 1 (2018) 1-20*
DOI: https://doi.org/10.12989/aae.2018.1.1.001

Optimization of ride comfort for a three-axle vehicle equipped with interconnected hydro-pneumatic suspension system

Ferhat Saglam*[1] and Y. Samim Unlusoy[2a]

[1]*ASELSAN Incorporation, Ankara, Turkey*
[2]*Middle East Technical University, Mechanical Engineering Department, Ankara, Turkey*

(Received January 26, 2017, Revised August 24, 2017, Accepted January 16, 2018)

Abstract. The aim of this study is the optimization of the parameters of interconnected Hydro-Pneumatic (HP) suspension system of a three-axle vehicle for ride comfort and handling. For HP suspension systems of equivalent vertical stiffness and damping characteristics, interconnected HP suspension systems increase roll and pitch stiffness and damping characteristics of the vehicle as compared to unconnected HP suspension systems. Thus, they result in improved handling and braking/acceleration performances of the vehicle. However, increased roll and pitch stiffness and damping characteristics also increase roll and pitch accelerations, which in turn result in degraded ride comfort performance. Therefore, in order to improve both ride comfort and vehicle handling performances simultaneously, an optimum parameter set of an interconnected HP suspension system is obtained through an optimization procedure. The objective function is formed as the sum of the weighted vertical accelerations according to ISO 2631. The roll angle, one of the important measures of vehicle handling and driving safety, is imposed as a constraint in the optimization study. Upper and lower parameter bounds are used in the optimization in order to get a physically realizable parameter set. Optimization procedure is implemented for a three-axle vehicle with unconnected and interconnected suspension systems separately. Optimization results show that interconnected HP suspension system results in improvements in both ride comfort and vehicle handling performance, as compared to the unconnected suspension system. As a result, interconnected HP suspension systems present a solution to the conflict between ride comfort and vehicle handling which is present in unconnected suspension systems.

Keywords: hydro-pneumatic suspension; interconnected suspension; ride comfort; vehicle handling; optimization; roll angle; three-axle vehicle

1. Introduction

In this study, optimization of the suspension parameters for a three-axle vehicle equipped with Hydro-Pneumatic (HP) suspension system for ride for comfort and handling is performed. As Fig. 1 shows, in its basic structure, HP suspension system consists of a gas volume, two oil volumes, floating piston, main piston, hydraulic cylinder and an orifice or damper valve. The gas volume provides HP suspension system with elasticity and flow of oil through the orifice or damper valve

∗Corresponding author, Ph.D., E-mail: fesaglam@gmail.com
[a]Professor, E-mail: unlusoy@metu.edu.tr

http://www.techno-press.org/?journal=csm&subpage=8 ISSN: 2234-2184 (Print), 2234-2192 (Online)

hydraulically interconnected suspension systems improved vehicle handling, yet they reduced vehicle ride comfort for a two-axle vehicle. Ding *et al.* (2012) studied the modelling of a three-axle vehicle with hydraulically interconnected mechanical suspension system in the pitch plane. The results showed that hydraulically interconnected suspension system improves the pitch motion without sacrificing ride comfort performance. Another potential use of the interconnected HP suspension system is to equalize or distribute the load among the axle group of heavy commercial vehicle. In the study of the Saglam and Unlusoy (2016b), an interconnected HP suspension system was studied for the rear axle group of a heavy commercial vehicle for load sharing purposes. Static and dynamic load sharing performance of the designed interconnected HP suspension system was examined by the simulations.

In the studies mentioned so far, the aim is the modelling and simulation of the vehicle with interconnected HP suspension system, and nominal parameter sets are used in simulations. In literature, there are also studies related to the optimization of the unconnected HP suspension system. Thoresson (2003) studied the optimization of the suspension system parameters of a two-axle off-road vehicle for ride comfort and handling. The parameters, damping characteristics scale coefficients, and the HP suspension gas volumes of the front and rear suspensions are optimized. Objection function for the vehicle ride comfort and handling was defined as the weighted root mean square (rms) of the vertical acceleration and body roll angle, respectively. Thoresson *et al.* (2009a, b) studied the modelling of a simplified vehicle ride and vehicle handling to be used in the vehicle suspension optimization and the full vehicle model in MSC ADAMS software. The simplified vehicle models were used for the gradient information and the full vehicle model was used for the objective function evaluation. Normalized HP suspension gas volumes and normalized damper scale factors were again used as the parameters to be optimized. Optimization was performed according to ride comfort, handling, and both ride comfort and handling. As expected, for handling optimization, gas volumes were set to the lower boundary values and damping values were set to upper boundary values. For ride comfort, gas volumes were set to upper boundary values and damping values were set to lower boundary values. For combined ride comfort and handling optimization, the damping values and gas volumes were set to values within the parameter space for compromised solution. Els and Uys (2003) studied the optimization of a HP suspension system for ride comfort and handling. Parameters of the suspension system, HP suspension gas volumes and damping scale factors, were optimized. The cost function to be minimized was formed as the weighted rms of the vertical acceleration in the Belgian paved road simulation, and the optimization constraint was formed as the maximum roll angle in the lane change simulation. Then, maximum roll angle was taken as the cost function and rms of the vertical acceleration was used as the optimization constraint. As the conclusion of the study, it was suggested that optimization should be performed for improved handling for better optimization results.

The literature survey shows the existence of studies on the optimization of unconnected HP suspension systems for ride comfort and vehicle handling. It is noted, however, that there is no published study related to the optimization of interconnected suspension system parameters of multi-axle vehicles for simultaneous ride comfort and vehicle handling. For unconnected suspension systems, the optimization results show that there is a compromise solution for ride comfort and vehicle handling. However, as will be explored in the following sections, by using the potential performance of the interconnected HP suspension system, it is possible to improve vehicle ride comfort and handling performances simultaneously.

In the following sections, modelling of the interconnected HP suspension system for a full

As Fig. 2 illustrates, all suspension units are interconnected to each other in the lateral and longitudinal directions by hydraulic conductors. Front left, front right, intermediate left, intermediate right, rear left, and rear right suspension forces are given as, Saglam (2016),

$$
\begin{aligned}
F_{FL} = {} & \frac{P_{30FL}V_{30FL}^{\kappa}A_p}{\left[V_{30FL}+A_p\left(z_{pFL}-z_{tFL}-\frac{A_{pr}}{A_p}\left(z_{pMR}-z_{tMR}\right)\right)\right]^{\kappa}}-\\
& -\frac{P_{30RR}V_{30RR}^{\kappa}A_{pr}}{\left[V_{30RR}+A_p\left(z_{pRR}-z_{tRR}-\frac{A_{pr}}{A_p}\left(z_{pFL}-z_{tFL}\right)\right)\right]^{\kappa}}-\\
& -A_p\left[\frac{A_p\left(\dot z_{pFL}-\dot z_{tFL}\right)-A_{pr}\left(\dot z_{pMR}-\dot z_{tMR}\right)}{A_vC_D}\right]^2\frac{\rho}{2}\mathrm{sign}\begin{bmatrix}A_p\left(\dot z_{pFL}-\dot z_{tFL}\right)-\\-A_{pr}\left(\dot z_{pMR}-\dot z_{tMR}\right)\end{bmatrix}+\\
& +A_{pr}\left[\frac{A_p\left(\dot z_{pRR}-\dot z_{tRR}\right)-A_{pr}\left(\dot z_{pFL}-\dot z_{tFL}\right)}{A_vC_D}\right]^2\frac{\rho}{2}\mathrm{sign}\begin{bmatrix}A_p\left(\dot z_{pRR}-\dot z_{tRR}\right)-\\-A_{pr}\left(\dot z_{pFL}-\dot z_{tFL}\right)\end{bmatrix}-\\
& -\frac{A_{pr}^2\left(\dot z_{pFL}-\dot z_{tFL}\right)}{R_{4FL1RR}}
\end{aligned}
\tag{1}
$$

$$
\begin{aligned}
F_{FR} = {} & \frac{P_{30FR}V_{30FR}^{\kappa}A_p}{\left[V_{30FR}+A_p\left(z_{pFR}-z_{tFR}-\frac{A_{pr}}{A_p}\left(z_{pML}-z_{tML}\right)\right)\right]^{\kappa}}-\\
& -\frac{P_{30RL}V_{30RL}^{\kappa}A_{pr}}{\left[V_{30RL}+A_p\left(z_{pRL}-z_{tRL}-\frac{A_{pr}}{A_p}\left(z_{pFR}-z_{tFR}\right)\right)\right]^{\kappa}}-\\
& -A_p\left[\frac{A_p\left(\dot z_{pFR}-\dot z_{tFR}\right)-A_{pr}\left(\dot z_{pML}-\dot z_{tML}\right)}{A_vC_D}\right]^2\frac{\rho}{2}\mathrm{sign}\begin{bmatrix}A_p\left(\dot z_{pFR}-\dot z_{tFR}\right)-\\-A_{pr}\left(\dot z_{pML}-\dot z_{tML}\right)\end{bmatrix}+\\
& +A_{pr}\left[\frac{A_p\left(\dot z_{pRL}-\dot z_{tRL}\right)-A_{pr}\left(\dot z_{pFR}-\dot z_{tFR}\right)}{A_vC_D}\right]^2\frac{\rho}{2}\mathrm{sign}\begin{bmatrix}A_p\left(\dot z_{pRL}-\dot z_{tRL}\right)-\\-A_{pr}\left(\dot z_{pFR}-\dot z_{tFR}\right)\end{bmatrix}-\\
& -\frac{A_{pr}^2\left(\dot z_{pFR}-\dot z_{tFR}\right)}{R_{4FR1RL}}
\end{aligned}
\tag{2}
$$

$$
\begin{aligned}
F_{ML} = {} & \frac{P_{30ML}V_{30ML}^{\kappa}A_p}{\left[V_{30ML}+A_p\left(z_{pML}-z_{tML}-\frac{A_{pr}}{A_p}\left(z_{pRR}-z_{tRR}\right)\right)\right]^{\kappa}}-\\
& -\frac{P_{30FR}V_{30FR}^{\kappa}A_{pr}}{\left[V_{30FR}+A_p\left(z_{pFR}-z_{tFR}-\frac{A_{pr}}{A_p}\left(z_{pML}-z_{tML}\right)\right)\right]^{\kappa}}-\\
& -A_p\left[\frac{A_p\left(\dot z_{pML}-\dot z_{tML}\right)-A_{pr}\left(\dot z_{pRR}-\dot z_{tRR}\right)}{A_vC_D}\right]^2\frac{\rho}{2}\mathrm{sign}\begin{bmatrix}A_p\left(\dot z_{pML}-\dot z_{tML}\right)-\\-A_{pr}\left(\dot z_{pRR}-\dot z_{tRR}\right)\end{bmatrix}+\\
& +A_{pr}\left[\frac{A_p\left(\dot z_{pFR}-\dot z_{tFR}\right)-A_{pr}\left(\dot z_{pML}-\dot z_{tML}\right)}{A_vC_D}\right]^2\frac{\rho}{2}\mathrm{sign}\begin{bmatrix}A_p\left(\dot z_{pFR}-\dot z_{tFR}\right)-\\-A_{pr}\left(\dot z_{pML}-\dot z_{tML}\right)\end{bmatrix}-\\
& -\frac{A_{pr}^2\left(\dot z_{pML}-\dot z_{tML}\right)}{R_{4ML1FR}}
\end{aligned}
\tag{3}
$$

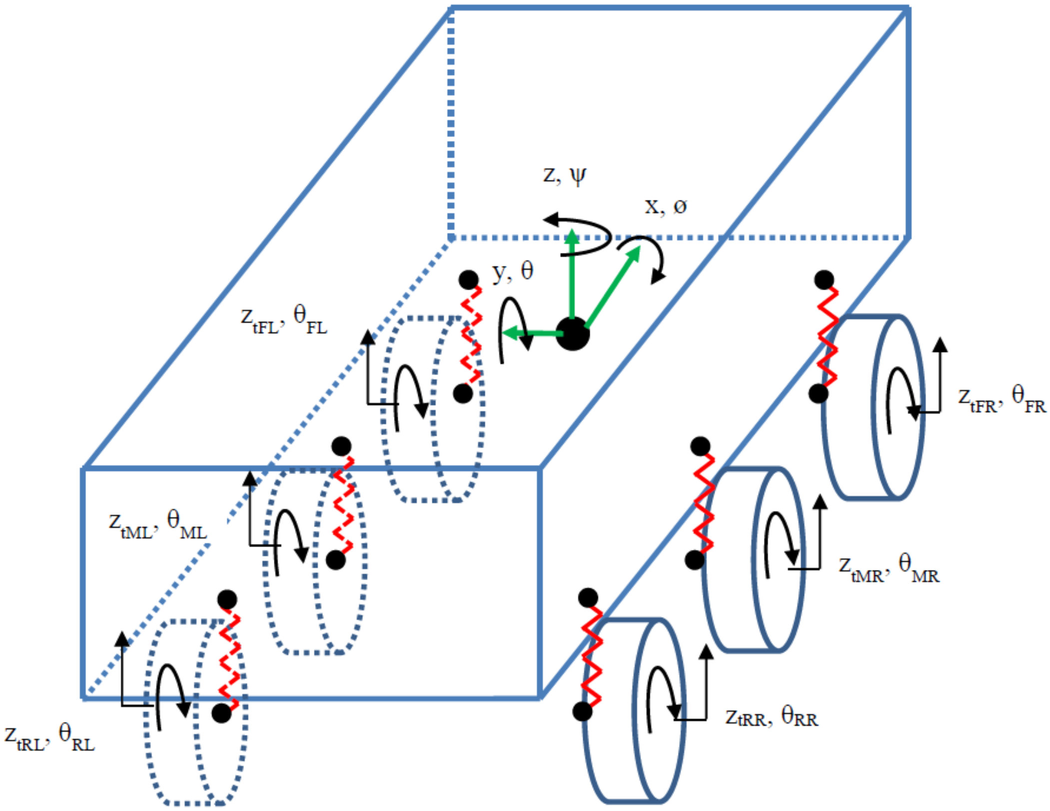

Fig. 3 Eighteen degree of freedom full vehicle model, Saglam and Unlusoy (2016a)

In these equations P_{30}'s are the initial gas pressures at static equilibrium, V_{30}'s are the initial gas volumes at static equilibrium, κ is the polytropic gas constant, z_p's are the piston displacement, z_t's are the tire displacement, A_p is the piston area, A_{pr} is the difference between the piston and piston rod area, A_v is the orifice opening area, C_D is the orifice damping loss factor, ρ is the oil density, and R_{41}'s are the hydraulic conductor resistance, and "FL", "FR", "ML", "MR", "RL", and "RR" stand for the front left, front right, intermediate left, intermediate right, rear left, and rear right, respectively.

The important characteristics of the interconnected suspension system is its ability to increase roll and pitch stiffness and damping characteristics without increasing the vertical stiffness and damping characteristics. For a vehicle with unconnected HP suspension configuration, the only way of increasing the roll and pitch stiffness and damping characteristics is to increase vertical stiffness and damping characteristic. In the study by Saglam and Unlusoy (2016a), roll and pitch stiffness and damping characteristics of the vehicles with unconnected and interconnected HP suspension systems were compared. It was concluded that when the vertical stiffness and damping characteristics of the vehicle with unconnected and interconnected HP suspension systems are equalized to each other, the vehicle with interconnected HP suspension system has higher roll and pitch stiffness and damping characteristics.

Interconnected HP suspension system is incorporated into the eighteen degree of freedom full vehicle model shown in Fig. 3, Saglam and Unlusoy (2016a). Full vehicle model consists of

vibration amplitude, direction, duration, and frequency content. According to the ISO 2631 standard, human exposure to vibrations can be evaluated in a quantitative manner by the so called reduced comfort boundaries. These reduced comfort boundaries provide the rms values of the limiting acceleration values in different directions for different exposure durations, and in a range of frequencies. Frequency shaping filters are commonly used to evaluate the results of vibration exposure. In the study by Zuo and Nayfeh (2003), low-order continuous time filter for the ride comfort frequency weighting curves given in Fig. 3 is obtained.

The third order mathematical representation of this filter shown is given as, (Zuo and Nayfeh 2003)

$$W_k(s) = \frac{80.03s^2 + 989.0s + 0.02108}{s^3 + 78.92s^2 + 2412s + 5614} \tag{7}$$

For the interconnected HP suspension system, the design parameters are initial gas volumes at static equilibrium, piston areas, orifice or damper valve parameters, and for the interconnected suspension system the piston rod areas. Among these parameters, piston and piston rod areas affect both suspension stiffness and damping. On the other hand, gas volumes only affect suspension stiffness, and orifice or valve parameters only affect suspension damping. By changing the piston area, oil and gas pressures can be tuned to physically realizable values. In order to simplify the optimization study, piston rod area is not included in optimized parameter set. The design parameters of the interconnected and unconnected HP suspension systems and the related suspension characteristics of the design parameters are summarized in Table 1.

Table 1 Design and optimized suspension parameters

	Suspension Design Parameters	Optimized Parameters
Stiffness	A_p, A_r, V_{30}	A_r, V_{30}
Damping	A_p, A_r, Orifice or Valve Parameters	A_r, Orifice or Valve Parameters

In optimization, instead of using these parameters directly, their normalized values are used. These normalized parameters are defined as,

$$n_{V30} = \frac{V_{30n}}{V_{30}} \tag{8}$$

$$n_{Damp} = \frac{c_n}{c} \tag{9}$$

$$n_{Ar} = \frac{A_{rn}}{A_p} \tag{10}$$

In these equations, n_{v30} represents the normalized gas volume, V_{30n} represents nominal gas volume, n_{Damp} represents normalized valve or orifice damping, c_n represents nominal valve or orifice characteristics, c represents valve or orifice damping, n_{Ar} represents normalized piston rod area, A_{rn} represents nominal piston rod area, and A_p represents piston area. In order to get

In these equations $W_k(k)$ is frequency filter which is given in Fig. 4 and, z_{FL}, z_{FR}, z_{ML}, z_{MR}, z_{RL}, z_{RR} are the vertical displacements of the sprung mass at different locations shown in Fig. 5 and ϕ is the roll angle. The positions of the vertical acceleration points are chosen as to represent the positions of the seats in the vehicle.

Before the optimization study, in order to see the effects of the optimized parameters on the vertical acceleration and the roll angle, a parametric study is conducted and then the optimization study is performed. For ride comfort evaluations, simulations are performed with random road displacement input. Power spectral densities of the random road displacement input at different forward speeds are given in Fig. 6. Similarly, lane change simulations are performed for the handling performance evaluations. Steering input for the lane change manoeuvre is shown in Fig. 7.

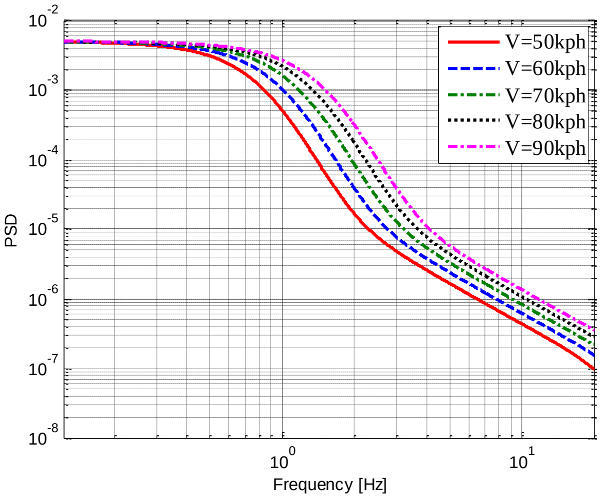

Fig. 6 Power spectral densities of random displacement inputs at different forward speeds

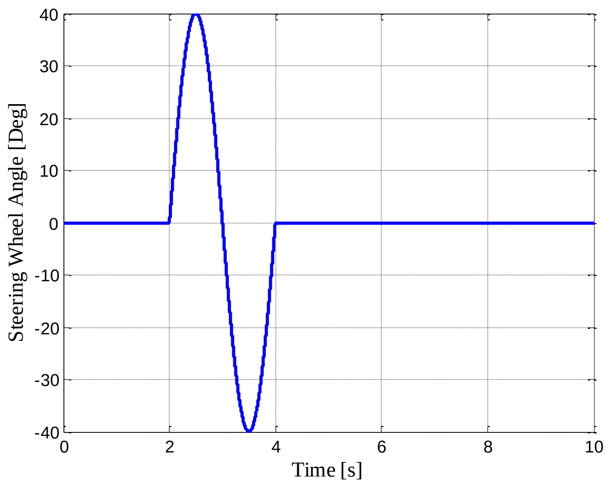

Fig. 7 Steering wheel input for lane change manoeuvre

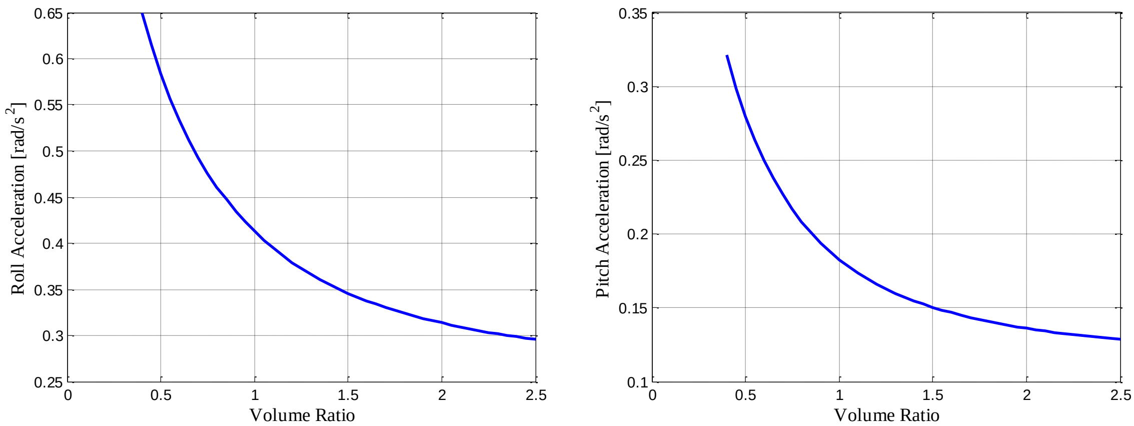

Fig. 9 rms of roll and pitch acceleration

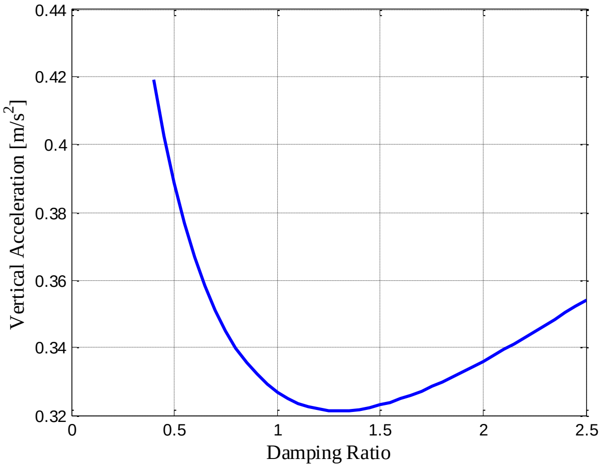

Fig. 10 rms of vertical acceleration

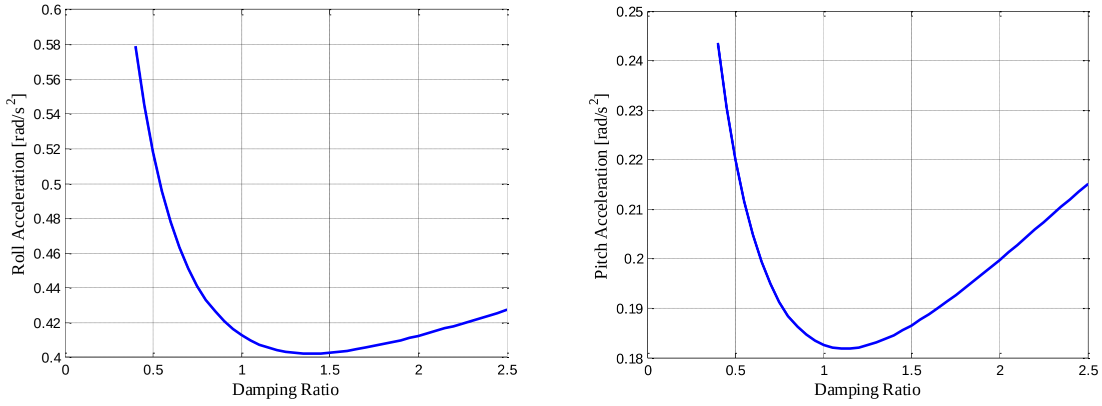

Fig. 11 rms of roll and pitch acceleration

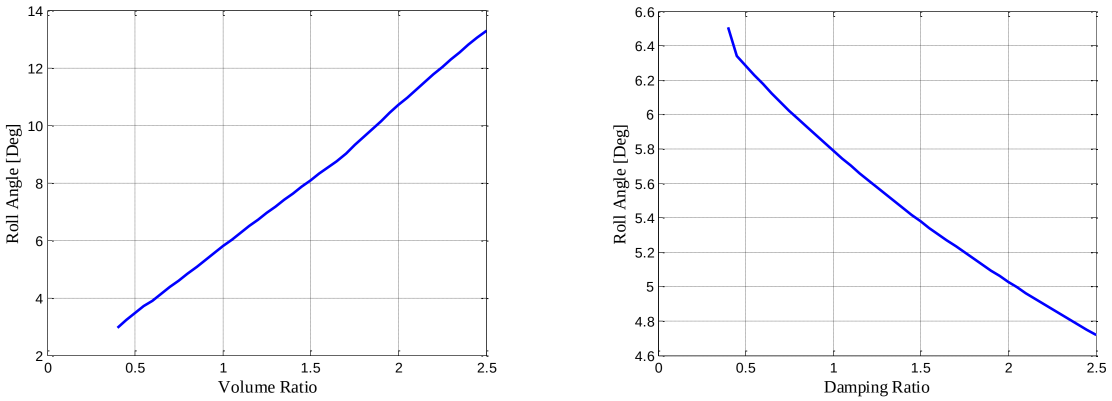

Fig. 14 roll angle vs. volume and damping ratio

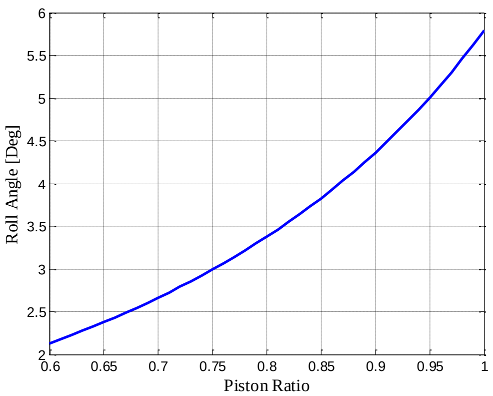

Fig. 15 roll angle vs. piston ratio

results in lower vertical ride comfort performance, and higher roll and pitch ride comfort performances.

Simulations are then performed with the lane change manoeuvre. Simulation results are shown in Figs. 14 and 15. The results show that, when the volume ratio is reduced the suspension stiffness increases, and the roll angle is reduced. When the damping ratio increases, maximum value of the roll angle decreases. The volume ratio has a stronger influence on the roll angle response than the damping ratio. When the piston ratio decreases, the roll stiffness increases, and the roll angle gets smaller.

In summary, as expected, making the suspension stiffer by reducing the gas volumes improves the vehicle handling, but degrades the vehicle ride comfort. When the piston ratio is decreased, vertical stiffness and damping are also decreased, yet roll stiffness and damping are increased. Therefore, there is a tendency of increasing ride comfort and vehicle handling performance simultaneously.

3.2 Optimization results

Table 6 Optimization results

	Ride Comfort (ϕ=8 Deg)			Handling (ϕ=4 Deg)		
	Uncon.	Intercon.	%	Uncon.	Intercon.	%
Acceleration (m/s^2)	0.77	0.46	40	1.00	0.48	52
Roll Angle (Deg)	7.7	5.0	35	4.0	3.9	3

Table 7 Optimum parameter sets for ride comfort optimization

	Unconnected	Interconnected
Parameter	Value	Value
Front Volume Ratio	1.00	2.45
Front Damping Ratio	1.61	0.76
Front Piston Rod Ratio	-	0.63
Intermediate Volume Ratio	1.47	2.45
Intermediate Damping Ratio	0.41	0.43
Intermediate Piston Rod Ratio	-	0.62
Rear Volume Ratio	2.50	2.50
Rear Damping Ratio	0.42	0.41
Rear Piston Rod Ratio	-	0.63

Table 8 Optimum parameter sets for handling optimization

	Unconnected	Interconnected
Parameter	Value	Value
Front Volume Ratio	0.50	2.39
Front Damping Ratio	2.50	1.28
Front Piston Rod Ratio	-	0.65
Intermediate Volume Ratio	0.44	1.82
Intermediate Damping Ratio	0.77	0.41
Intermediate Piston Rod Ratio	-	0.61
Rear Volume Ratio	2.50	2.47
Rear Damping Ratio	0.41	0.50
Rear Piston Rod Ratio	-	0.60

maximum roll angle of the vehicle with the unconnected suspension system.

For the improved handling behaviour of the vehicle, 4 degrees roll angle constraint is imposed during the optimization. As Table 5 illustrates, the vehicle with the interconnected HP suspension system has a somewhat higher volume ratio and lower damping ratio. These parameters result from the need to lower the vertical acceleration and thus increasing the ride comfort. However, the piston rod area is again set to its lower limit in order to reduce the roll angle. For the vehicle with the unconnected HP suspension system, a low value of the volume ratio and a high value of the damping ratio are obtained in order to limit the roll angle to 4 degrees. Thus, the suspension stiffness is increased, and thus ride comfort is degraded. Since the vehicle with the interconnected

parameters in order to get a physically realizable parameter set. In the optimization, genetic algorithm is used. Optimization is performed for two different vehicle performance characteristics, first of which is the improved ride comfort, and the second is the improved vehicle handling, for both the unconnected and interconnected HP suspension systems.

According to the optimization results, the vehicle with the interconnected HP suspension system has better ride comfort and handling performances with respect to vehicle with the unconnected HP suspension system. For the unconnected HP suspension system, the roll angle is lowered by reducing gas volumes and by increasing the suspension damping, which degrades the ride comfort. However, for the interconnected HP suspension system, the roll angle can be reduced by reducing the piston rod area. Therefore, suspension stiffness and damping in the vertical direction do not have to be increased, so that ride comfort is not affected. As a result, vehicle with the interconnected HP suspension system provides an alternative solution to the inherent conflict between vehicle ride and handling characteristics improvement.

Note

This paper is revised and expanded version of a paper entitled "Optimization of ride comfort for a three-axle vehicle equipped with interconnected hydro-pneumatic suspension system" presented at OTEKON2016, 8. Automotive Technologies Congress, Bursa, 23-24 May, 2016.

References

Bauer, W. (2011), *Hydropneumatic Suspension Systems*, Springer, Heidelberg.

Cao, D. (2008), "Theoretical analyses of roll- and pitch-coupled hydro-pneumatic strut suspensions", Ph.D. Dissertation, Concordia University, Canada.

Chong, E.K.P. and Zak, S.H. (2008), *An Introduction to Optimization*, 3rd Edition, Wiley-Interscience.

Ding, F., Han, X., Luo, Z. and Zhang, N. (2012), "Modeling and characteristic analysis of tri-axle trucks with hydraulically interconnected suspensions", *Vehic. Syst. Dyn.: Int. J. Vehic. Mech. Mobil.*, **50**(12), 1877-1904.

Els, P.S. and Uys, P.E. (2003), "Investigation of the applicability of the dynamic-Q optimization algorithm to vehicle suspension design", *Math. Comput. Model.*, **37**(9-10), 1029-1046.

ISO, International Organization for Standardization (1977), *ISO 2631: Evaluation of Human Exposure to Whole-Body Vibration*.

Joo, F.R. (1991), "Dynamic analysis of a hydropneumatic suspension system", M.Sc. Dissertation, Concordia University, Canada.

Saglam, F. (2016), "Optimization of ride comfort for vehicles equipped with passive and active hydro-pneumatic suspensions", Ph.D. Dissertation, Middle East Technical University, Turkey.

Saglam, F. and Unlusoy, Y.S. (2014), "Modeling and state dependent riccati equation control of an active hydro-pneumatic suspension system", *Proceedings of the International Conference of Control, Dynamic Systems, and Robotics*, Ottawa, Canada, May.

Saglam, F. and Unlusoy, Y.S. (2016a), "Modelling and simulation of a three-axle vehicle with interconnected hydro-pneumatic suspension system", *Proceedings of the Fisita World Automotive Congress*, Busan, Korea, September.

Saglam, F. and Unlusoy, Y.S. (2016b), "Analysis of interconnected hydro-pneumatic suspension system for load sharing among heavy vehicle axles", *Proceedings of the 3rd International Conference on Control, Dynamic Systems, and Robotics*, Ottawa, Canada, May.

Smith, W.A., Zhang, N. and Hu, W. (2011), "Hydraulically interconnected vehicle suspension: Handling performance", *Vehic. Syst. Dyn.: Int. J. Vehic. Mech. Mobil.*, **49**(1-2), 87-106.
Smith, W.A., Zhang, N. and Jeyakumaran, J. (2010b), "Hydraulically interconnected vehicle suspension: Theoretical and experimental ride analysis", *Vehic. Syst. Dyn.: Int. J. Vehic. Mech. Mobil.*, **48**(1), 41-64.
The Mathworks Inc. (2013), *Matlab Global Optimization Toolbox, Genetic Algorithm*.
Thoresson, M.J. (2003), "Mathematical optimization of the suspension system of an off-road vehicle for ride comfort and handling", M.Sc. Dissertation, University of Pretoria, Pretoria, South Africa.
Thoresson, M.J., Uys, P.E. and Snyman, J.A. (2009), "Efficient optimization of a vehicle suspension system using a gradient-based approximation method, part 1: Mathematical modelling", *Math. Comput. Model.*, **50**(9-10), 1421-1436.
Thoresson, M.J., Uys, P.E. and Snyman, J.A. (2009), "Efficient optimization of a vehicle suspension system using a gradient-based approximation method, part 2: Optimization results", *Math. Comput. Model.*, **50**(9-10), 1437-1447.
Zhang, N., Smith, W.A. and Jeyakumaran, J. (2010a), "Hydraulically interconnected vehicle suspension: Background and modeling", *Vehic. Syst. Dyn.: Int. J. Vehic. Mech. Mobil.*, **48**(1), 17-40.
Zuo, L. and Nayfeh, S.A. (2003), "Low order continuous-time filters for approximation of the ISO-2631-1 human vibration sensitivity weightings", *J. Sound Vibr.*, **265**(2), 459-465.

FO